

## Molecular Docking and Spectroscopic Analysis of (Z)-3-(3-chloro-2,6-difluorophenyl)-1-(1H-imidazol-1-yl)prop-2-en-1-one

K. Kumanan<sup>1</sup>, R. Raj Muhamed<sup>1\*</sup>, M. Raja<sup>2</sup>, V. Sathyanarayanamoorthi<sup>3</sup>, M. Yaseen Mowlana<sup>4</sup>, S. Arulappan<sup>1</sup>

<sup>1</sup>Department of Physics, Jamal Mohamed College, Tiruchirappalli 620020, Tamil Nadu, India.

<sup>2</sup>Department of Physics, Govt Thirumagal Mills College, Gudiyattam 632602, Vellore, India.

<sup>3</sup>Department of Physics, PSG College of Arts and Science, Coimbatore 641014, Tamil Nadu, India.

<sup>4</sup>Department of Chemistry, Jamal Mohamed College, Tiruchirappalli 620020, Tamil Nadu, India.

Corresponding Author: ponnu\_68@yahoo.com

### Abstract

Theoretical and experimental FT-IR and FT-Raman spectra characterization of 2(Z)-3-(3-chloro-2,6-difluorophenyl)-1-(1H-imidazol-1-yl)prop-2-en-1-one were recorded and calculated. The vibrational wavenumbers were computed using DFT quantum chemical calculations. The molecular geometry (bond length, bond angle) and vibrational frequencies of the title compounds have been calculated by using DFT/B3LYP method with 6-311++G(d,p) basis set. The title compounds were screened in vitro for antimicrobial activity against three bacterial and three fungal strains. Molecular docking studies reveal that title compound play a vital role in bonding and results draw us to the concluded that title compound inhibit different antimicrobial proteins and that have good biological activities.

**Keywords:** DFT; FTIR; FT-Raman; Antimicrobial; Molecular docking.

### 1. Introduction

The imidazole nucleus is well known to play an important role in living organisms since it is incorporated into the histidine molecule and many other important biological systems. Imidazole derivatives are the most used class of antifungal drugs [1], being active against

pathogenic and nonpathogenic fungi [2]. Particularly, imidazole and its derivative of (Z)-3-(3-chloro-2,6-difluorophenyl)-1-(1H-imidazol-1-yl)prop-2-en-1-one have broadened scope in clinical medicines. Its molecular formula is  $C_{12}H_7ClF_2N_2O$ . Medicinal properties of imidazoles include anti-inflammatory, anticancer, anticoagulants, antifungal, antibacterial, antitubercular, antiviral, antimalarial and antidiabetic [3,4]. In the present work has been undertaken to give a complete description of the molecular geometry and molecular vibration of the 3CDIPO.

In the present work has been undertaken to give a complete description of the molecular geometry and molecular vibration of the 3CDIPO. FTIR and Raman spectra of (Z)-3-(3-chloro-2,6-difluorophenyl)-1-(1H-imidazol-1-yl)prop-2-en-1-one (3CDIPO) have been reported together with the assignments of the vibrational modes supported by PED. The agar diffusion methods were used to study the antimicrobial activity of the title compound against three bacteria (Moraxella, Enterobacter and Pseudomonas aeruginosa), and three fungi organisms (Candida albicans, A.niger and Trichophyton) and the title showed a broad spectrum of activities against the microbes. Due to the different potential biological

activity of the title compound, molecular docking of the title compound is also reported.

## 2. Material and Methods

### 2.1. Synthesis

For the synthesis of ((Z)-3-(3-chloro-2,6-difluorophenyl)-1-(1H-imidazol-1-yl)prop-2-en-1-one (3CDIPO) compound, Equimolar quantity of 1-acetyl imidazole (0.01 mol) and 3-chloro-2,6-difluorobenzaldehyde (0.01 mol) were dissolved in 20 ml of ethanol in a 150 mL round bottomed flask. The reaction mixture was magnetically stirred for 3h in ice-cold condition, during stirring 10 ml of 10% sodium hydroxide solution was added drop wise. A flocculants precipitate was formed. The precipitate was filtered and washed with cold water. The solid obtained was purified by column chromatography using silica gel 60-120 mesh and n-hexane: acetone (7:3 v/v) as eluate. The reaction scheme is shown in Figure 1.

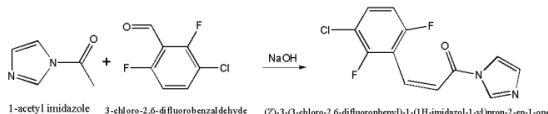


**Figure 1.** The scheme of the synthesis of 3CDIPO

### 2.2. Experimental details

The FT-IR spectrum of the synthesis compound ((Z)-3-(3-chloro-2,6-difluorophenyl)-1-(1H-imidazol-1-yl)prop-2-en-1-one (3CDIPO) was recorded in the region 4000-450  $\text{cm}^{-1}$  in evacuation mode using a KBr pellet technique with 1.0  $\text{cm}^{-1}$  resolution on a PERKIN ELMER FT-IR spectrophotometer. The FT-Raman spectrum of the 3CDIPO compound was recorded in the region 4000-100  $\text{cm}^{-1}$  in a pure mode using Nd: YAG Laser excitation wavelength of Raman 100 mW with 2  $\text{cm}^{-1}$  resolution on a BRUCKER RFS 27 at SAIF, IIT, Chennai, India.

### 2.3. Computational details

In this work, all the calculations were performed by using Gauss-View molecular visualization program [5] and Gaussian 09 W program package [6]. Molecular docking (ligand-protein) simulations have been performed by using autoDock 4.2.6 software package.

## 3. Results and discussion

### 3.1. Geometrical structure analysis

The optimized geometry is performed at B3LYP/6-311++G(d,p) basis set of 3CDIPO molecule with atom numbering scheme is shown in Figure 2. The theoretical results are compared with related molecule such as (Z)-3-(9-Anthryl)-1-(4-chlorophenyl)-2-(4-nitro-1H-imidazol-1-yl)prop-2-en-1-one [7]. The comparative optimized structural parameters such as bond length, bond angle along with its experimental data's are presented in Table 1. This title molecule has ten C – C bond lengths, seven C – H bond lengths, five C – N bond lengths, two C – F bond lengths, one (C – O) bond length presented in title molecule and these values are listed in Table 1. From table 1 shows the calculated and experimental results are very good agreement. So the title molecule optimized successfully.

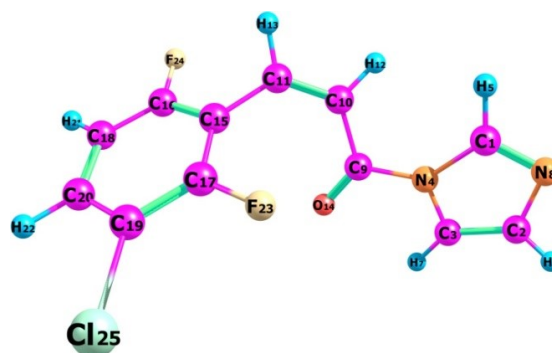


**Figure 2.** The theoretical optimized geometric structure with atoms numbering of 3CDIPO

### 3.2. FT-IR and FT-Raman spectra

The maximum number of potentially active observable fundamentals of a nonlinear molecule which contains N atoms is equal to (3N-6), apart from three translational and three rotational degrees of freedom. Hence, 3CDIPO molecule, that was planar, has 25 atoms with 69 normal modes of vibrations. The observed and simulated infrared and Raman spectra of 3CDIPO are shown in Figs. 3 and 4, respectively. The observed and scaled theoretical frequencies using DFT (B3LYP) method with PEDs are listed in Table 2.

The C-C stretching vibrations are expected in the range from 1650 to 1100  $\text{cm}^{-1}$  which are not significantly influenced by the nature of the substituents [8]. The C-C stretching vibrations of the 3CDIPO compound were observed from 1670 to 890  $\text{cm}^{-1}$ . In this present study, the C-C stretching vibrations are found at 1568(vs), 1597(vs), 1444(vs), 1235(vs), 1162(vs), 1067(s), 938(m)  $\text{cm}^{-1}$  in FT-IR and 1647(s), 1595(vs), 1415(s), 1177(w), 1104(m), 973(w), 947(m), 905(m)  $\text{cm}^{-1}$  in FT-Raman respectively. The theoretical wavenumbers at 1697, 1583, 1443, 1411, 1239, 1190, 1146, 1100, 1080, 989, 944 and 891  $\text{cm}^{-1}$  are assigned as C-C stretching vibrations with PED contribution of 68, 46, 24, 63, 34, 24, 30, 25, 22, 21, 25 and 36% respectively.

**Table 1.** Optimized geometrical parameters of 3CDIPO obtain by B3LYP/6-311++G(d,p) basis set

| Parameters     | Exp <sup>a</sup> | B3LYP/        | Parameters   | Exp <sup>a</sup> | B3LYP |
|----------------|------------------|---------------|--------------|------------------|-------|
| Bond length(Å) |                  | Bond angle(°) |              |                  |       |
| C1-N4          | 1.364            | 1.391         | N4-C1-H5     | 123.9            | 122.6 |
| C1-H5          | 0.930            | 1.078         | N4-C1-N8     | 112.2            | 111.9 |
| C1-N8          | 1.305            | 1.301         | C1-N4-C3     | 106.9            | 106.0 |
| C2-C3          | 1.357            | 1.361         | C1-N4-C9     | 128.0            | 129.7 |
| C2-H6          | 0.930            | 1.078         | H5-C1-N8     | 127.9            | 125.5 |
| C2-N8          | 1.369            | 1.389         | C1-N8-C2     | 106.9            | 105.6 |
| C3-N4          | 1.369            | 1.393         | C3-C2-H6     | 127.9            | 128.0 |
| C3-H7          | 0.930            | 1.075         | C3-C2-N8     | 112.8            | 110.9 |
| N4-C9          | 1.431            | 1.418         | C2-C3-N4     | 104.2            | 105.6 |
| C9-C10         | 1.488            | 1.483         | C2-C3-H7     | 127.9            | 133.4 |
| C9-O14         | 1.216            | 1.210         | H6-C2-N8     | 123.9            | 121.1 |
| C10-C11        | 1.341            | 1.342         | N4-C3-H7     | 123.9            | 120.9 |
| C10-H12        | 0.930            | 1.083         | C3-N4-C9     | 125.0            | 124.3 |
| C11-H13        | 0.930            | 1.086         | N4-C9-C10    | 116.1            | 115.6 |
| C11-C15        | 1.477            | 1.470         | N4-C9-O14    | 118.1            | 119.9 |
| C15-C16        | 1.402            | 1.399         | O14-C9-O14   |                  | 124.4 |
| C15-C17        | 1.402            | 1.400         | C9-O14-C11   |                  | 125.4 |
| C16-C18        | 1.384            | 1.382         | C9-C10-H12   | 115.3            | 116.9 |
| C16-F24        |                  | 1.352         | C11-C10-H12  | 119.7            | 117.5 |
| C17-C19        | 1.402            | 1.391         | C10-C11-H13  | 115.3            | 116.6 |
| C17-F23        |                  | 1.339         | C10-C11-C15  | 129.4            | 129.4 |
| C18-C20        | 1.402            | 1.391         | H13-C11-C15  | 115.3            | 114.1 |
| C18-H21        | 0.930            | 1.082         | C11-C15-C16  | 119.6            | 119.6 |
| C19-C20        | 1.402            | 1.392         | C11-C15-C17  | 123.4            | 124.4 |
| C19-Cl25       |                  | 1.744         | C16-C15-C17  | 117.3            | 115.9 |
| C20-H22        | 0.930            | 1.082         | C15-C16-C18  | 123.5            | 123.6 |
|                |                  |               | C15-C16-F24  |                  | 117.7 |
|                |                  |               | C15-C17-C19  | 122.4            | 122.1 |
|                |                  |               | C15-C17-F23  |                  | 118.9 |
|                |                  |               | C18-C16-C24  | 118.8            | 118.7 |
|                |                  |               | C16-C18-C20  | 118.6            | 118.6 |
|                |                  |               | C16-C18-H21  | 119.8            | 119.8 |
|                |                  |               | C19-C17-F23  |                  | 118.9 |
|                |                  |               | C17-C19-C20  | 119.6            | 119.6 |
|                |                  |               | C17-C19-Cl25 |                  | 119.8 |
|                |                  |               | C20-C18-H21  | 120.7            | 121.6 |
|                |                  |               | C18-C20-C19  | 120.4            | 120.2 |
|                |                  |               | C18-C20-H22  | 120.5            | 120.5 |
|                |                  |               | C20-C19-Cl25 |                  | 120.6 |
|                |                  |               | C19-C20-H22  | 119.3            | 119.3 |

<sup>a</sup> Taken from Ref [13]

In the heterocyclic compounds, the C-H stretching wavenumbers appear in the range 3000-3100  $\text{cm}^{-1}$  [9]. In this present study, the C-H stretching vibrations are observed at 3166, 3122, 3090 and 3031  $\text{cm}^{-1}$  by B3LYP/6-311++G(d,P) method show good agreements with experimental vibrations. The bands observed in the recorded

FT-Raman spectrum 3163(w), 3106(m), 3082(m) and 3034(w)  $\text{cm}^{-1}$ . The PED corresponding to this

pure mode of title molecule contributed 95, 94, 97 and 92% is shown in Table 2.

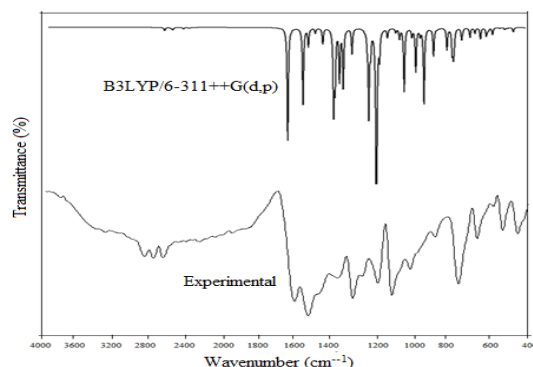


**Figure 3.** Experimental and theoretical FT-IR spectra of 3CDIPO

**Table 2.** Calculated vibrational frequencies ( $\text{cm}^{-1}$ ) assignments of 3CDIPO based on B3LYP/6-311++G(d,p) basis set

| Mode no | Experimental wave number ( $\text{cm}^{-1}$ ) |          | Theoretical wave number ( $\text{cm}^{-1}$ ) |        | $I_{\text{IR}}^c$ | $I_{\text{RAMAN}}^d$ | Assignments (PED) <sup>a,b</sup>                    |
|---------|---|----------|--|--------|-------------------|----------------------|---|
|         | FTIR  | FT-Raman | Unscaled                                     | Scaled |                   |                      |   |
| 69      |   |          | 3295   | 3166   | 1                 | 7                    | $\gamma$ CH(95)                                     |
| 68      |   |          | 3259   | 3132   | 0                 | 5                    | $\gamma$ CH (96)                                    |
| 67      |   | 3106(m)  | 3248   | 3122   | 1                 | 13                   | $\gamma$ CH (94)                                    |
| 66      |   | 3082(m)  | 3215   | 3090   | 0                 | 22                   | $\gamma$ CH (97)                                    |
| 65      |   |          | 3203   | 3078   | 0                 | 6                    | $\gamma$ CH (97)                                    |
| 64      |   |          | 3186   | 3062   | 1                 | 11                   | $\gamma$ CH (91)                                    |
| 63      |   |          | 3154   | 3031   | 0                 | 7                    | $\gamma$ CH (92)                                    |
| 62      | 1668(vs)                                      | 1647(s)  | 1765   | 1697   | 49                | 9                    | $\gamma$ CC (68)                                    |
| 61      |   |          | 1678   | 1612   | 34                | 100                  | $\gamma$ CC(40)+ $\beta$ HCN (14)                   |
| 60      | 1597(vs)                                      | 1595(vs) | 1647   | 1583   | 8                 | 19                   | $\gamma$ CC (46)                                    |
| 59      |   | 1513(m)  | 1607   | 1544   | 2                 | 3                    | $\beta$ HCC (31)                                    |
| 58      |   |          | 1564   | 1503   | 7                 | 3                    | $\gamma$ CC (60)                                    |
| 57      | 1444(vs)                                      |          | 1502   | 1443   | 35                | 4                    | $\beta$ HCN(14)+ $\gamma$ NC(31) + $\gamma$ CC (24) |
| 56      |   |          | 1493   | 1435   | 23                | 1                    | $\beta$ HCC(26)                                     |
| 55      |   | 1415(s)  | 1468   | 1411   | 23                | 8                    | $\gamma$ CC (63)                                    |
| 54      | 1365(vs)                                      | 1376(w)  | 1447   | 1390   | 26                | 3                    | $\beta$ HCC(19)+ $\beta$ HCN(10)                    |
| 53      | 1317(s)                                       |          | 1396   | 1342   | 11                | 1                    | $\beta$ HCN(42) + $\gamma$ NC (12)                  |
| 52      |   |          | 1324   | 1272   | 1                 | 3                    | $\gamma$ CC (61)                                    |
| 51      |   |          | 1309   | 1258   | 5                 | 6                    | $\gamma$ NC (45) + $\beta$ CNC(20)                  |
| 50      |   |          | 1300   | 1249   | 38                | 4                    | $\gamma$ CC (36)                                    |
| 49      | 1235(vs)                                      |          | 1289   | 1239   | 8                 | 8                    | $\beta$ HCN (12) + $\gamma$ CC (34)                 |
| 48      |   | 1218(w)  | 1267   | 1217   | 1                 | 3                    |   |
| 47      |   |          | 1256   | 1207   | 100               | 1                    | $\beta$ HCN (15) + $\gamma$ (13)                    |
| 46      |   | 1177(w)  | 1238   | 1190   | 11                | 0                    | $\gamma$ CC(24) + $\beta$ HCC (24)                  |
| 45      | 1162(vs)                                      |          | 1193   | 1146   | 4                 | 2                    | $\beta$ HCC (11) + $\gamma$ CC (14)                 |
| 44      |   | 1104(m)  | 1145   | 1100   | 2                 | 1                    | $\beta$ HCC (20) + $\gamma$ CC (10)                 |

| Mode no | Experimental wave number (cm <sup>-1</sup> ) |          | Theoretical wave number (cm <sup>-1</sup> ) |        | I <sub>IR</sub> <sup>c</sup> | I <sub>RAMAN</sub> <sup>d</sup> | Assignments (PED) <sup>a,b</sup>                       |
|---------|--|----------|---|--------|------------------------------|---------------------------------|--|
|         | FTIR   | FT-Raman | Unscaled                                    | Scaled |                              |                                 |  |
| 43      | 1067(s)                                      |          | 1124  | 1080   | 4                            | 1                               | $\gamma$ NC (37) + $\gamma$ CC (12) + $\beta$ HCN (12) |
| 42      |  |          | 1096  | 1054   | 28                           | 6                               | $\beta$ HCN (36)+ $\gamma$ CC (27)                     |
| 41      |  | 1021(w)  | 1052  | 1011   | 4                            | 0                               | $\gamma$ NC (30)                                       |
| 40      |  |          | 1030  | 989    | 19                           | 1                               | $\gamma$ CC (21)                                       |
| 39      |  |          | 1005  | 966    | 3                            | 7                               | $\tau$ HCCN (38)                                       |
| 38      | 938(m)                                       | 947(w)   | 983   | 944    | 33                           | 1                               | $\gamma$ CC (25)+ $\beta$ HCN (12)                     |
| 37      |  |          | 948   | 911    | 0                            | 0                               | $\tau$ HCCCI (68)+ $\tau$ HCCF (15)                    |
| 36      |  |          | 927   | 891    | 12                           | 1                               | $\gamma$ CC (36)                                       |
| 35      |  |          | 908   | 872    | 1                            | 1                               | $\beta$ HCN (63)                                       |
| 34      |  | 855(w)   | 893   | 858    | 0                            | 0                               | $\tau$ HCCH (90)                                       |
| 33      | 816(vs)                                      |          | 851   | 817    | 9                            | 1                               | $\gamma$ CC (10)+ $\beta$ HCC (10)                     |
| 32      |  |          | 820   | 788    | 10                           | 0                               | $\tau$ HCCC (70)                                       |
| 31      |  |          | 813   | 782    | 10                           | 0                               | $\tau$ HCNC (76)                                       |
| 30      |  |          | 809   | 777    | 6                            | 4                               |  |
| 29      |  | 745(w)   | 766   | 736    | 5                            | 0                               | $\tau$ HCNC (53)                                       |
| 28      | 718(m)                                       |          | 760   | 730    | 1                            | 1                               | $\tau$ HCNC (21)                                       |
| 27      |  |          | 718   | 690    | 4                            | 1                               | $\gamma$ CC (14)                                       |
| 26      |  | 669(w)   | 690   | 663    | 2                            | 0                               | $\tau$ HCCO (24)                                       |
| 25      | 633(w)                                       | 633(w)   | 658   | 632    | 5                            | 0                               | $\tau$ HCNC (49)                                       |
| 24      |  |          | 624   | 600    | 4                            | 1                               |  |
| 23      |  |          | 618   | 594    | 1                            | 0                               | $\tau$ HCCC (28)                                       |
| 22      | 586(w)                                       |          | 611   | 588    | 1                            | 3                               | $\tau$ HCNC (11)                                       |
| 21      |  |          | 588   | 565    | 3                            | 0                               | $\gamma$ CC (10) + $\tau$ HCCC (11)+ $\beta$ HCC (10)  |
| 20      | 508(w)                                       |          | 547   | 525    | 0                            | 0                               | $\beta$ HCC (25)                                       |
| 19      |  |          | 518   | 498    | 1                            | 1                               |  |
| 18      |  |          | 502   | 483    | 0                            | 0                               | $\tau$ HCCC (10) + $\tau$ HCCO (18)                    |
| 17      |  | 437(w)   | 470   | 451    | 2                            | 0                               | $\beta$ HCC (39)                                       |
| 16      |  |          | 400   | 384    | 0                            | 3                               | $\tau$ HCCC (18)                                       |
| 15      |  | 377(w)   | 381   | 366    | 1                            | 1                               | $\beta$ HCC (35) + $\tau$ HCCC (12) + $\gamma$ CC (13) |
| 14      |  | 346(w)   | 349   | 335    | 0                            | 0                               | $\beta$ CNC (10)                                       |
| 13      |  |          | 331   | 318    | 0                            | 0                               | $\tau$ HCCF (51)                                       |
| 12      |  |          | 304   | 292    | 4                            | 0                               | $\beta$ HCC (12)                                       |
| 11      |  |          | 271   | 260    | 0                            | 1                               | $\tau$ HCCC (19)                                       |
| 10      |  | 205(w)   | 245   | 235    | 0                            | 0                               | $\beta$ CCC (35)                                       |
| 9       |  |          | 201   | 193    | 0                            | 0                               | $\tau$ HCNC (11)                                       |
| 8       |  |          | 157   | 151    | 0                            | 0                               | $\beta$ HCC (10)+ $\tau$ HCNC (14)                     |
| 7       |  |          | 149   | 143    | 1                            | 0                               | $\tau$ HCNC (54)                                       |
| 6       |  |          | 124   | 119    | 0                            | 0                               | $\tau$ HCCCI (64)                                      |
| 5       |  | 107(w)   | 115   | 110    | 1                            | 1                               | $\tau$ HCCN (11)+ $\tau$ HCCC (24)                     |
| 4       |  | 72(w)    | 82  | 79     | 0                            | 0                               | $\tau$ HCCC (14)                                       |
| 3       |  |          | 49  | 47     | 0                            | 0                               | $\tau$ HCCN (11) + $\tau$ HCCC (22)                    |
| 2       |  |          | 38  | 37     | 0                            | 1                               | $\beta$ HCC (11) + $\tau$ HCCC (11)                    |
| 1       |  |          | 17  | 16     | 0                            | 0                               | $\tau$ HCCN (30)                                       |

<sup>a</sup> $\gamma$ -stretching,  $\beta$ - bending ,  $\tau$ -torsion, vs-very strong, s- strong, m-medium, w-weak, vw-very weak.

<sup>b</sup>scaling factor : 0.961 for B3LYP/6-311+G(d,p)

<sup>c</sup>Relative absorption intensities normalized with highest peak absorption equal to 100.

<sup>d</sup>Relative Raman intensities normalized to 100.

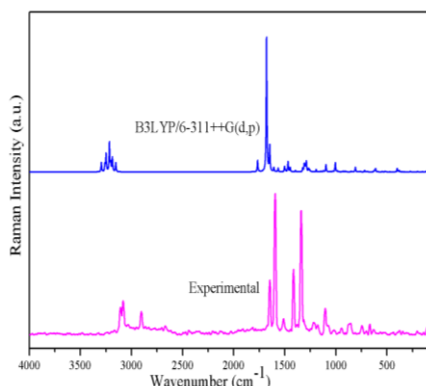


**Figure 4.** Experimental and theoretical FT-Raman spectra of 3CDIPO

### 3.3. Antimicrobial studies

The title compound have been examined for in-vitro antibacterial activity against three bacterial strains such as, Moraxella, Enterobacter, Pseudomonas aeruginosa and three fungal strains such as, Candida albicans, A.niger and Trichophyton, which were selected for the present investigation by agar-disk diffusion method. Antimicrobial (antibacterial and antifungal) activity of DMSO extracts with different concentration (25, 50, 75 and 100  $\mu$ l) inhibition Zone (mm) in agar well diffusion method is tabulated in Table 3.

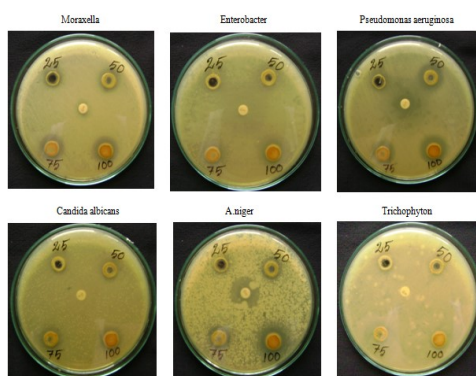


**Figure 5.** Antibacterial activity and antifungal activity of title molecule

Title compound is more active Moraxella, Enterobacter, Pseudomonas aeruginosa, Candida

albicans, A.niger and Trichophyton compared than standard drug. Together, these results indicate that 3CDIPO shows broad-spectrum antimicrobial activity against. The activities of 3CDIPO against bacterial and fungal pathogens are shown in Figure5.

**Table 3.** Antimicrobial activity of 3CDIPO

| Organism               | DMSO Extract added and Zone of inhibition (mm/ml) |            |            |            |             |
|------------------------|---|------------|------------|------------|-------------|
|                        | Control   | 25 $\mu$ l | 50 $\mu$ l | 75 $\mu$ l | 100 $\mu$ l |
| Moraxella              | 11  | 12         | 15         | 17         | 19          |
| Enterobacter           | 25  | 15         | 19         | 22         | 26          |
| Pseudomonas aeruginosa | 25  | 12         | 15         | 16         | 20          |
| Candida albicans       | 13  | 13         | 15         | 18         | 20          |
| A.niger                | 20  | 12         | 15         | 18         | 25          |
| Trichophyton           | 10  | 12         | 15         | 20         | 24          |

### 3.4. Molecular docking

The molecular docking is used to predict the preferred binding orientation, binding energy and activity of molecules and their protein targets. The aim to investigate the binding mode, a molecular modeling study was performed and 3CDIPO was selected to be docked into the active site of three receptors 3F03, 4UM7 and 4HOE of antimicrobial proteins.

The AutoDockTools graphical user interface [10] was used to remove the ligand and water molecules present in the target proteins. The first rank docking parameters such as binding energy, inhibition constant and intermolecular energy of the molecule with respect to the targeted proteins are listed in Table 4. The preferred binding orientation of the 3CDIPO ligand with respect to the target proteins are represented in Figs. 6-8. In Figure 6-8, the yellow line indicates the formation of intermolecular hydrogen bond between 3CDIPO

ligand and the proteins. These results indicate that the 3CDIPO ligand exhibits the lower binding energy and inhibition constant for the targeted protein associated with the 3F03 compared with the other targeted proteins associated with the 4UM7, 4HOE. Among them, 3F03 exhibited the lowest free energy at -6.50 kcal/mol and most docked inhibitors interacted with the ligand within the 3F03 binding site. They exhibited up to two hydrogen bonds involving ARG 324 and ARG 324 with RMSD being 8.79 Å. The docking simulation shows the best binding mode of the 3CDIPO into 3F03. These findings confirm that the 3CDIPO molecule can act as a good inhibitor against 3F03.

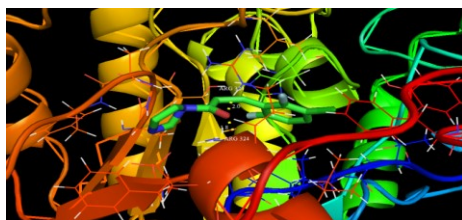


**Figure 6.** Docking and Hydrogen bond interactions 3CDIPO with 3F03 protein structure

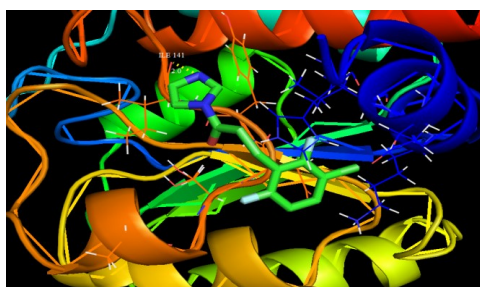


**Figure 7.** Docking and Hydrogen bond interactions 3CDIPO with 4UM7 protein structure

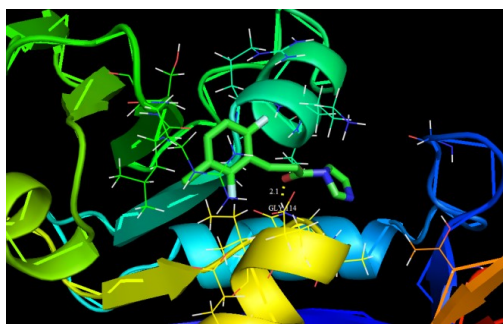


**Figure 8.** Docking and Hydrogen bond interactions 3CDIPO with 4HOE protein structure

**Table 4.** Hydrogen bonding and molecular docking with antimicrobial protein targets

| Protein (PDB ID) | Bonded residues | No. of hydrogen bond | Bond distance (Å) | Estimated Inhibition Constant ( $\mu\text{m}$ ) | Binding energy (kcal/mol) | Reference RMSD (Å) |
|------------------|-----------------|----------------------|-------------------|---|---------------------------|--------------------|
| 3F03             | ARG 324         | 2                    | 2.0               | 17.15   | -6.50                     | 8.79               |
|                  | ARG 324         |                      | 1.8               |   |                           |                    |
| 4UM7             | ILE 141         | 1                    | 2.0               | 245.72  | -4.92                     | 21.75              |
| 4HOE             | GLY 114         | 1                    | 2.1               | 17.20   | -6.48                     | 33.45              |

#### 4. Conclusion

The investigation of the present work is illuminate the spectroscopic properties such as molecular parameters, frequency assignments and electronic transition and of title compound by using FTIR, FT-Raman and tools derived from the density functional theory. Due to the lack of experimental information on the structural parameters available in the literature, the optimized geometric parameters (bond lengths and bond angles) was theoretically determined at B3LYP/6-311++G(d,p) level of theory and compared with the structurally similar compound. The vibrational FT-IR and FT-Raman spectra of the 3CDIPO were recorded and computed vibrational wavenumbers and their PED were calculated.

#### References

- [1] Bell, A.S., Triazole antifungals: Itraconazole (Sporanox), fluconazole (Diflucan), Voriconazole (Vfend) and fosfluconazole (Prodif), In The Art of Drug Synthesis, 5 (2007)72–73.2
- [2] Narasimhan, B., Sharma, D., Kumar, P., Biological importance of the imidazole nucleus in the new millennium. Med. Chem. Res. 20 (2011) 1119-1140.



- [3] Congiu, C., Cocco, M.T., Onnis, V., Design, synthesis and in vitro antitumor activity of new 1, 4-diarylimidazole-2-ones and their 2-thione analogues. *Bioorg Med Chem Lett* 18 (2008) 989–993.
- [4] Siddiqui, I.R., Singh, P.K., Srivastava, V., Singh, J., Facile synthesis of acyclic analogues of carbocyclic nucleoside as potential anti-HIV pro-drug. *Indian Journal of Chemistry* 49B (2010) 512-520.
- [5] GaussView, Version 5, Roy Dennington, Todd Keith, and John Millam, Semichem Inc., Shawnee Mission, KS, 2009.
- [6] Frisch, M.J., Trucks, G.W., Schlegel, H.B., Scuseria, G.E., Robb, M.A. Gaussian 09, Revision E.01, Gaussian, Inc., Wallingford CT, 2009
- [7] Wang, G.Z., Lu, Y.H., Zhou, C.H., Zhang, Y.Y., (Z)-3-(9-Anthryl)-1-(4-chlorophenyl)-2-(4-nitro-1H-imidazol-1-yl)prop-2-en-1-one, *Acta Cryst.* E65 (2009) o1113.
- [8] Sundaraganesan, N., Illakiamani, S. Meganathan, C., Joshua, B.D., Vibrational spectroscopy investigation using ab initio and density functional theory analysis on the structure of 3-aminobenzotrifluoride, *Spectrochim. Acta A* 67 (2007) 214-224.
- [9] Swarnalatha, N., Gunasekaran, S., Muthu, S., Nagarajan, M. Molecular structure analysis and spectroscopic characterization of 9-methoxy-2H-furo[3,2-g]chromen-2-one with experimental (FT-IR and FT-Raman) techniques and quantum chemical calculations, *spectrochim. Acta part A* 137 (2015) 721-729.
- [10] Morris, G.M., Goodsell, D.S., Halliday, R.S., Huey, R., Hart, W.E., Belew, R.K., Olson, A.J., *J. Comput. Chem.* 19 (1998) 1639–1662.